SCIENTIFIC REPORTS

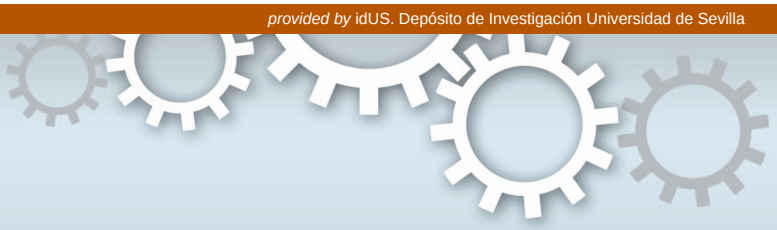

OPEN

SUBJECT AREAS:

SUPER-RESOLUTION MICROSCOPY

TECHNICAL REPORT

Received
10 July 2013

Accepted
27 September 2013

Published
14 October 2013

Correspondence and requests for materials should be addressed to J.V. (fvilladiego@us.es)

Direct confocal acquisition of fluorescence from X-gal staining on thick tissue sections

Konstantin L. Levitsky[1], Juan José Toledo-Aral[1,2,3], José López-Barneo[1,2,3] & Javier Villadiego[1,2,3]

[1]Instituto de Biomedicina de Sevilla (IBiS), Hospital Universitario Virgen del Rocío/CSIC/Universidad de Sevilla, Sevilla, Spain, [2]Departamento de Fisiología Médica y Biofísica, Facultad de Medicina, Universidad de Sevilla. Sevilla, Spain, [3]Centro de Investigación Biomédica en Red sobre Enfermedades Neurodegenerativas (CIBERNED), Spain.

X-gal staining is a common procedure used in the histochemical monitoring of gene expression by light microscopy. However, this procedure does not permit the direct confocal acquisition of images, thus preventing the identification of labelled cells on the depth (Z) axis of tissue sections and leading sometimes to erroneous conclusions in co-localization and gene expression studies. Here we report a technique, based on X-gal fluorescence emission and mathematically-based optical correction, to obtain high quality fluorescence confocal images. This method, combined with immunofluorescence, makes it possible to unequivocally identify X-gal-labelled cells in tissue sections, emerging as a valuable tool in gene expression and cell tracing analysis.

Reporter genes are used to monitor gene expression during embryonic development and in the postnatal period. Among the different reporter systems, X-gal staining (also referred to as LacZ staining) has emerged as an optimal choice based on its simplicity and high sensitivity. This procedure has been used to image gene expression in a large battery of LacZ-fused knockout mice as well as in the ROSA-26 strain of Cre-reporter expression[1]. X-gal staining is based on the presence of the bacterial LacZ gene that encodes for the β-galactosidase (β-gal) enzyme. The most common substrate used is 5-bromo-4-chloro-3-indolyl β-D-galactopyraniside (X-gal), which produces a dark blue precipitate that can be easily detected by light microscopy[2–5]. However, the use of light transmitted microscopy to detect X-gal staining does not permit localization of the precipitate in a defined confocal plane on tissue sections. This makes it difficult to precisely define whether or not a reporter gene is expressed in a particular cell within a complex tissue, despite combining the detection of the X-gal with immunolabelling of other cell markers, producing a significant amount of incorrect co-localization on thick tissue sections. Previous attempts to circumvent this major limitation have been based on the use of specific antibodies against β-gal[4]. However, X-gal staining is considerably less costly and, as it is based on an enzymatic reaction, offers a lower detection threshold and a better signal to noise ratio than immunofluorescence, which makes this histological method the first-choice technique to visualize low levels of gene expression. Here, we describe a simple method to obtain high quality fluorescence confocal images directly from X-gal-stained tissue sections. This technique of direct confocal acquisition of fluorescence from X-gal staining is based on the fact that the X-gal precipitate is able to absorb light in 570–700 nm range, and emit fluorescence in the 650–770 nm wavelength range. Importantly, the procedure is totally compatible with classical immunofluorescence, allowing a combination of the LacZ reporter system with multiple fluorescent labels.

Results

To investigate the possibility that X-gal precipitate can produce fluorescence emission, we purified X-gal from LacZ-expressing *E.coli* and analysed its absorption and emission spectra. We detected a peak of absorption in the 570–700 nm range (Fig. 1A) and studied whether, after absorption, the precipitate could emit a fluorescence signal. Indeed, after excitation of the X-gal precipitate at 633 nm we detected an emission signal in the 650–770 nm range (Fig. 1B). This finding makes it possible to obtain a fluorescence image using regular confocal microscopy. Figure 1C shows an image of purified X-gal precipitate as seen by regular light microscopy, while Fig. 1D illustrates images obtained from the same purified X-gal precipitate visualized by light-transmitted microscopy (left panel) and by fluorescence confocal microscopy (right panel) after excitation at 633 nm, which produces a high-resolution fluorescence image that was recorded in the 650–770 nm wavelength range. We did

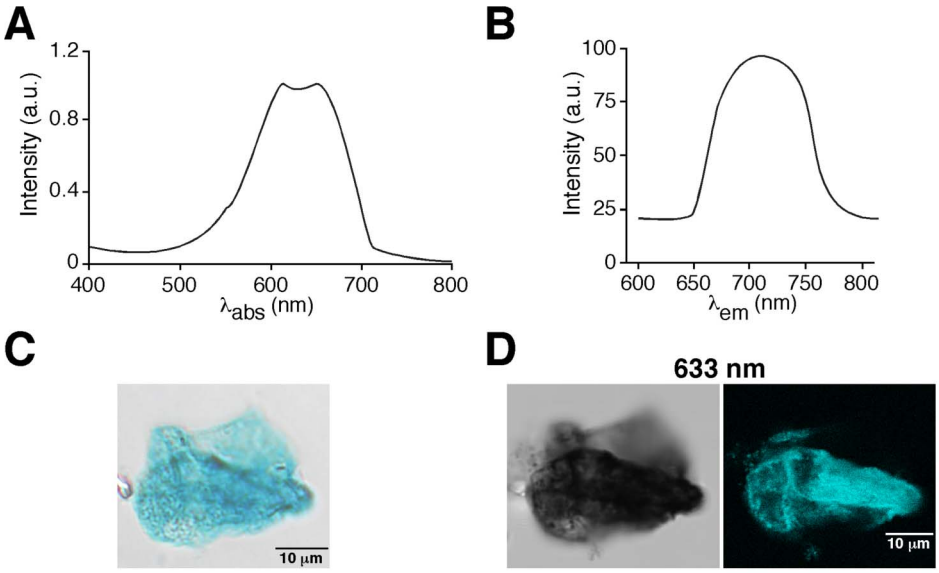

Figure 1 | X-gal fluorescence emission after excitation at 633 nm. (A). Absorption spectrum of X-gal. Note the peak of absorption in the 570–700 nm range. λ_{abs} = absorption light wavelength in nanometers. (B). Fluorescence emission spectrum of X-gal after excitation at 633 nm showing fluorescence emission in the 650–770 nm range; a.u: arbitrary units, λ_{em} = emitted light wavelength in nanometers. (C). Light microscopy image from purified X-gal precipitate deposited on a coverslip. (D). Images obtained from the same purified X-gal precipitate showed in C visualized by light transmitted microscopy (left panel) and by fluorescence confocal microscopy (right panel) after excitation with a wavelength of 633 nm.

not detect any fluorescent signal from the same X-gal precipitate with excitation wavelengths ranging from 405 to 561 nm (Supplementary Fig. 1).

The procedure described above (excitation at 633 nm and recording fluorescence emission in the 650–770 nm range) was subsequently tested on X-gal-stained tissue sections. Figure 2A shows two X-gal precipitates on a 30 μm thick brain section from a GDNF/X-gal[6,7] mouse visualized by regular light microscopy (left panel) and by light transmission microscopy (right panel) after illumination with a Helium-Neon 633 nm laser. Although both X-gal precipitates were clearly detected by light microscopy, this approach does not permit localization of the precipitate in a defined confocal plane in the depth (Z) axis. We excited the tissue section at 633 nm and recorded emitted fluorescence 650–770 nm range of a Z-stack (7.56 μm) obtaining confocal images that revealed two fluorescent dots perfectly coincident with the X-gal precipitates but in two

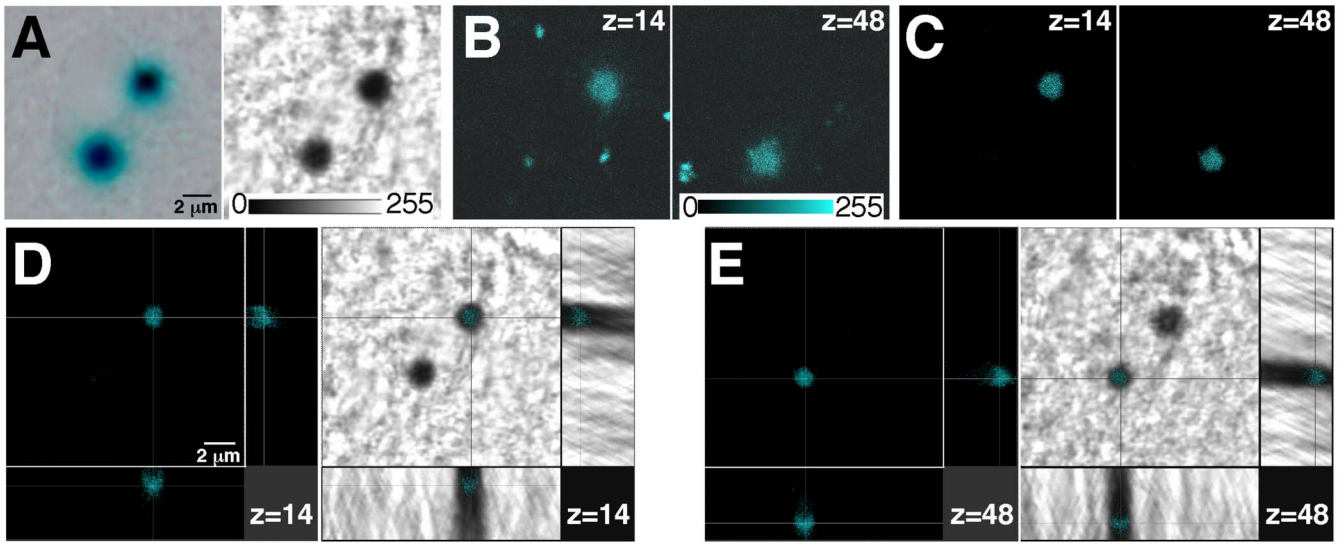

Figure 2 | Confocal acquisition of fluorescence from X-gal staining on thick tissue sections. (A). X-gal inclusions in a brain coronal section from a GDNF/LacZ mouse, visualized using regular light microscopy (left panel) or by light transmission microscopy after illumination at 633 nm in a confocal microscope (right panel). (B). Confocal acquisition of fluorescence (from a 7.56 μm Z-stack, voxel depth of 0.12 μm and pinhole of 1 airy) of the X-gal inclusions in A after excitation at 633 nm. Although both X-gal precipitates seem to appear in the same Z-plane in A (light microscopy), they are actually located in completely different Z-planes (z = 14 in left panel and z = 48 right panel; see scale of transmittance and fluorescence values in A and B). (C). Images shown in B after application of the mathematically-based optical correction procedure to eliminate background fluorescence: subtraction of the transmittance values after excitation at 633 nm from the fluorescence digital image. (D,E). Cross-section of the previously shown confocal-z-planes (z = 14 in D; and z = 48 in E) illustrating the x-y-z coincidence of the fluorescence signal (left panels) with the X-gal inclusion (right panels, visualized by light transmission microscopy).

different depth (Z) axis planes separated by ~4 μm [Fig 2B; Z = 14 in the left panel and Z = 48 in the right panel; voxel depth of 0.12 μm (Z-depth resolution of confocal planes) and pinhole 1 airy unit]. Although excitation of X-gal deposits allows the acquisition of a fluorescence signal that is clearly coincident with the X-gal precipitate, it produces a significant level of background fluorescence in the non-X-gal-labelled surrounding tissue (note the small fluorescence signals not coincident with the X-gal precipitates in Fig. 2B). This background signal, sometimes appearing as defined structures, could be due to auto-fluorescence of the neural tissue in the recorded wavelength range. Indeed, auto-fluorescence emission, on this range wavelength, by lysosomal lipofuscin has been reported[8]. Background noise could be increased by the high gain of the photomultiplier necessary to acquire the weak fluorescence emission from the X-gal precipitates. To improve the signal to noise ratio, we designed a mathematically-based optical correction method that significantly reduces the background fluorescence. This procedure consists of the simultaneous recording of the fluorescence and light transmitted signals by their respective photomultipliers once the tissue section has been excited at 633 nm. Both the fluorescence and light transmitted images are digitized using, for instance, an 8-bit scale (see scale values in Fig. 2A and B). The digitized values of transmittance are then subtracted from the fluorescence image values, resulting in high-resolution confocal images of fluorescence from the X-gal inclusions (Fig. 2C; left, Z = 14 and right Z = 48). Since X-gal precipitates are opaque, with transmittance values close to 0 (full absorbance), and the surrounding biological tissue is sufficiently clear to provide high values of transmittance (see relative scale of transmittance values showed in Fig. 2A), this correction procedure significantly reduces the level of the non-specific signal from the non-X-gal-labelled tissue without an accompanying loss of signal from the precipitate. Importantly, the transmittance values should be acquired after excitation of the sample at 633 nm because this wavelength produces the most opaque image of the X-gal precipitate from the different wavelengths tested. Thus, higher differences in the transmittance values between the opaque X-gal inclusions and the clear, non-labelled tissue, are obtained (see Fig. 1D transmitted light panel). The combination of the X-gal fluorescence emission with the optical correction method allows one to obtain high quality X-gal fluorescence confocal images which are perfectly coincident with the X-gal inclusion (Fig. 2D,E), thus making possible the unequivocal localization of the X-gal precipitate in a definite x-y-z position on thick tissue sections.

The described procedure is particularly relevant for analysing sections from complex tissues composed of different cell types that may be in close contact. A significant advantage of the direct fluorescent confocal acquisition of X-gal staining method is its compatibility with the emission range (~400–620 nm) of most common fluorophores used in immunohistochemical studies, hence making possible the combination of the LacZ reporter system with other antigens or fluorescent dyes. To further illustrate the performance of this new approach, we applied the confocal X-gal fluorescence detection to 30 μm-thick neostriatal sections from a GDNF/X-gal mouse; the sections were labelled with markers for interneurons (parvalbumin-Alexa

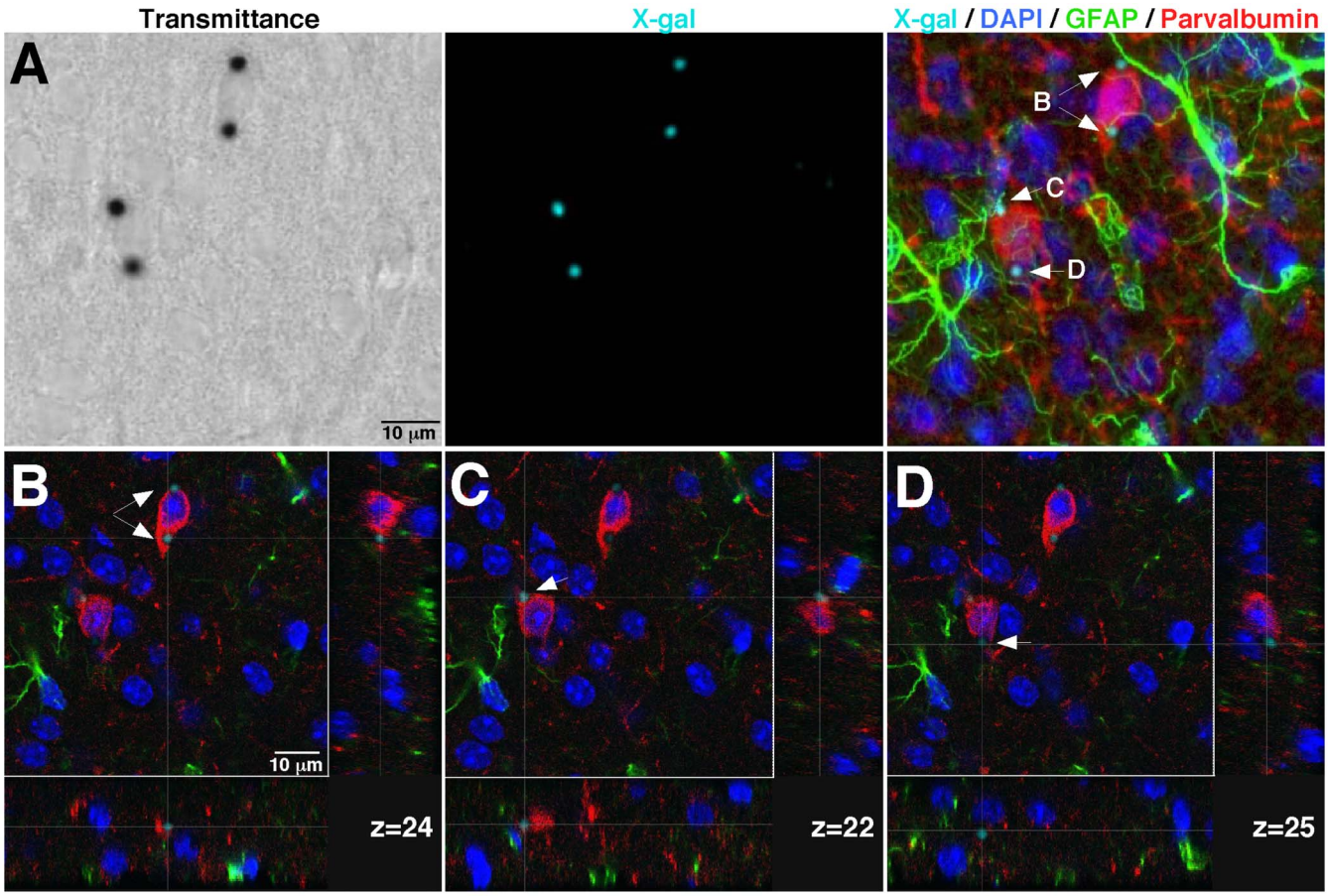

Figure 3 | Compatibility of the confocal acquisition of fluorescence from X-gal staining with multiple fluorescence labeling. (A). Transmittance image after illumination at 633 nm (left panel) and the maximal fluorescent projection images from X-gal (central panel) and merged fluorescence (X-gal/DAPI/GFAP/parvalbumin; right panel) obtained by confocal acquisition of a Z-stack of a 25.4 μm-thick of a GDNF/LacZ brain section after X-gal staining and immunofluorescence. (B–D). Cross-sections of the confocal-z-planes (voxel depth of 0.488 μm) in which each X-gal fluorescent dot in F (marked by arrows; right panel) are located.

568 nm excitation wavelength), astrocytes (glial fibrillary acid protein, GFAP-Alexa 488 nm excitation wavelength) and nuclei (4′,6′-diamidino-2-phenylindole, DAPI). Figure 3A shows the transmittance image after excitation at 633 nm (left panel) together with the maximal projection images of X-gal (central panel) and merged fluorescence (X-gal/DAPI/GFAP/parvalbumin; right panel) obtained by confocal acquisition (25.4 μm Z-stack, 0.48 μm voxel depth and pinhole of 1 airy). The merged fluorescence image (Fig. 3A, right panel) reveals X-gal fluorescence dots (arrows B, C and D) that, as shown in a previous report[9], seem to be inside parvalbumin-positive neurons, in very close contact with GFAP-positive glial processes (arrows B and C), or even outside of the neuronal soma (arrow D). Detailed inspection of the Z-confocal planes corresponding to each X-gal fluorescence dot revealed unequivocally that the X-gal deposits are produced by parvalbumin-positive neurons (Fig. 3B–D). Notably, X-gal fluorescence dots shown in Fig. 3C,D are located within the same neuron but appear in different z-confocal planes (z = 22 in Fig. 3C and z = 25 in Fig. 3D; separated in the depth (Z) axis by ~1.5 μm; see also Supplementary Fig. 2 illustrating the X-gal image processing operations). These images reveal that our method not only has sufficient resolution to localize the X-gal precipitate in a particular cell but also within subcellular structures of thick tissue sections. Note that this technique is particularly useful to decipher erroneous cases of apparent co-localization of X-gal precipitates in thick tissue sections. Figure 4A–C shows a typical analysis of co-localization by classical light transmitted/fluorescence microscopy of a coronal brain section after X-gal staining, DARPP32 immunofluorescence and nuclear staining with DAPI. Blue X-gal dots (labelled by arrowheads) seem to appear within a medium spiny, DARPP32-positive, cell, which is the neuronal class most abundant in the neostriatum. However, the analysis of the cross-sections of specific confocal-z-planes (Fig. 4D, z = 15; Fig. 4E, z = 19 and Fig. 4F, z = 8; and Supplementary Fig. 3 showing the X-gal image processing operations) of the same region using our method clearly reveals the absence of co-localization between the DARPP32-positive neurons and the X-gal dots. Therefore our procedure of direct confocal acquisition of fluorescence from X-gal staining is critical to avoid misinterpretation of classical light transmitted/fluorescence microscopy images due to the impossibility of localizing the X-gal signal in a defined depth (Z) plane.

Images shown in previous figures were obtained from the GDNF/X-gal mouse line, in which the expression of the β-gal enzyme is under the control of the endogenous GDNF promoter. This reporter mouse line shows a characteristic X-gal staining on neural tissue, presenting discrete X-gal deposits due to the low level of expression of the β-gal enzyme[7,9–11]. We also tested the validity of our method in a high-expression LacZ reporter line using a TH-ires-Cre/R26R mouse (carrying the Rosa26R-LacZ reporter construct). Figure 5A,B shows a coronal brain section from a TH-ires-Cre/R26R mouse after

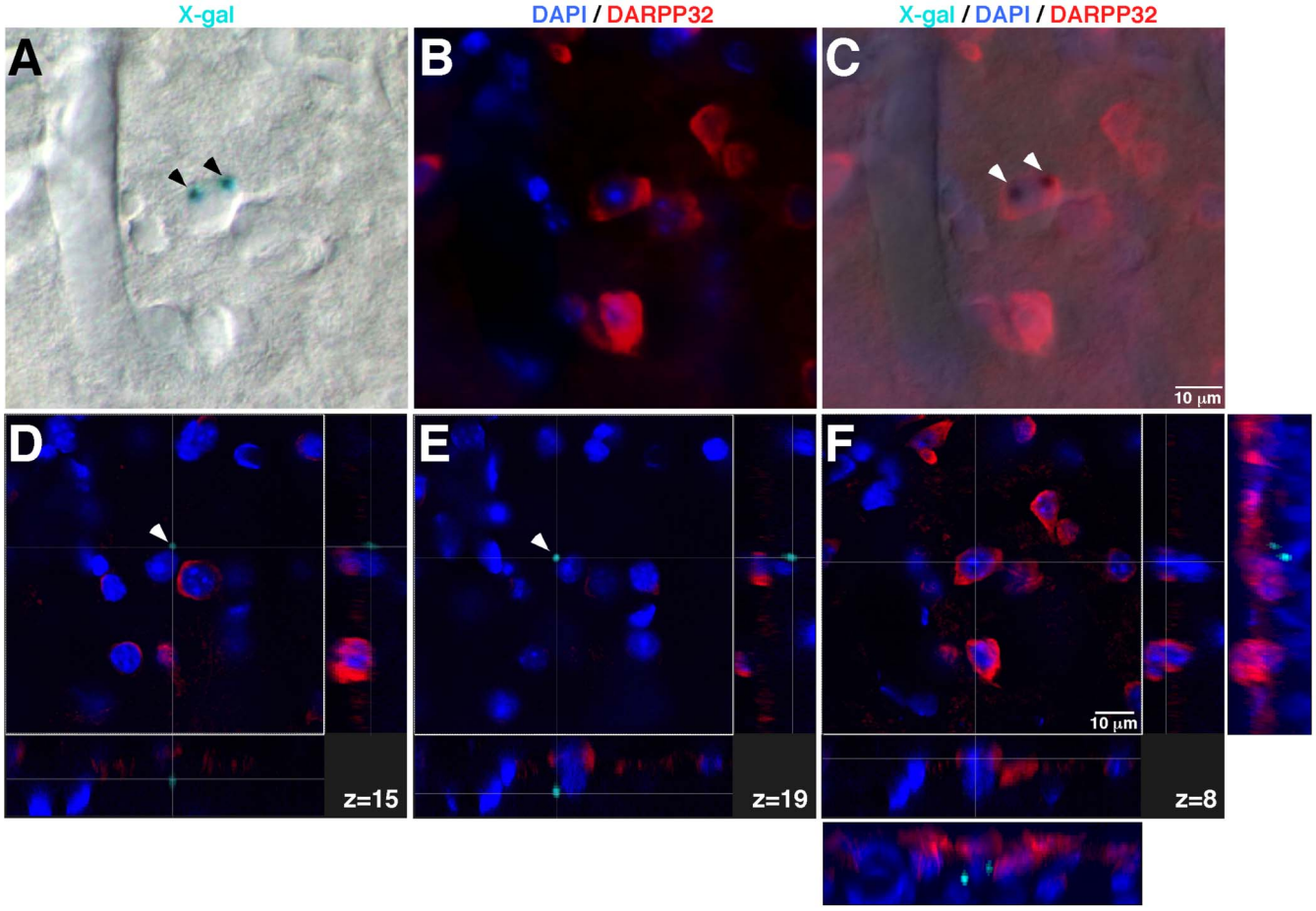

Figure 4 | Comparison between light transmitted/fluorescence microscopy and direct fluorescent confocal acquisition in the analysis of complex and misleading X-gal optical images. A–C. Light transmitted (A), fluorescence (B) and the merged image (C) of a coronal brain section after X-gal staining, DARPP32 immunofluorescence and nuclear staining with DAPI. Blue X-gal dots (labelled by arrowheads) seem to appear coincident with a DARPP32-positive neuron. (D–F). Cross-sections of specific confocal-z-planes (D, z = 15; E, z = 19 and F, z = 8) of the same region analysed in A–C, revealing the absence of co-localization between the DARPP32-positive neurons and the X-gal dots. Note the lateral views after 3D-reconstuction, adjacent to panel F, showing that the fluorescent X-gal dots do not correspond with any DARPP32-positive neuron. Confocal acquisition from a 20.0 μm Z-stack, voxel depth of 0.8 μm and pinhole airy 1.

X-gal staining and visualization by classical light transmitted microscopy (Fig. 5A) and 633 nm illumination (Fig. 5B). As expected, this LacZ reporter line shows high levels of X-gal labelling distributed throughout the soma of mesencephalic dopaminergic TH^+ neurons (Fig. 5A,B,D). In addition, some disperse X-gal inclusions also appeared as sparse dots that could be attributed to low levels of β-gal activity on TH^+ neuronal processes (see Fig. 5D). The confocal images showed in Fig. 5C,D clearly illustrate that the fluorescent X-gal signal are coincident with the X-gal staining revealed by classical light transmitted microscopy (Fig. 5A,B,D; and Supplementary Fig. 4 showing the X-gal image processing operations). Moreover, the fluorescent confocal X-gal label perfectly matches with the soma of TH^+ neurons as revealed by TH immunofluorescence (Fig. 5E–I). Interestingly, high magnification confocal images reported in Fig. 5G,I indicated that the disperse X-gal inclusions were inside dopaminergic TH^+ neuronal fibres. These experiments illustrate that the direct confocal acquisition of fluorescence from X-gal staining could be performed on cells or tissues with high level of β-gal activity, facilitating the co-localization analysis by the use of multiple fluorescent labelling. Moreover, this method emerges as an excellent tool to localize and clearly identify cells or subcellular structures that present low levels of β-gal expression or activity.

Discussion

In this paper we report a simple technique to perform direct confocal acquisition of fluorescence from X-gal staining. The possibility to obtain confocal images from X-gal staining has been previously reported by using near-infrared photoactivation (720–730 nm) of the X-gal precipitate with a Titanium-doped Saphire (Ti:S) laser[12]. However, the method presented here, combined with mathematically-based optical correction, allows high quality confocal images to be obtained from the X-gal-stained sections with the aid of a regular confocal microscope (fitted with a Helium-Neon 633 nm laser) without photoactivation, being totally compatible with the use of most common fluorescent dyes for immunolabelling. As part of our methodology we have also designed a mathematically-based optical correction protocol, which is the first description of a reliable method to significantly increase the signal to noise ratio for weak fluorescence.

The LacZ gene is widely used as a reporter system in different organisms, including a broad spectrum of genetically modified mouse lines. Here, we have presented an easy to implement and practical procedure to perform the confocal acquisition of fluorescence from X-gal-stained sections, which solves a major limitation of this reporter system. The new methodology unequivocally localizes the X-gal precipitates in defined depth (Z) focal planes and can be combined with multiple fluorescent labelling, thus alluding to its use as a valuable tool in gene expression and cell tracing studies. Interestingly, since senescence-associated beta-galactosidase activity has been widely used as biomarker of senescent cells[13], the method described here could be also applied to evaluate cell senescence in tissue or tumor sections. In addition, the fluorescent property of X-gal makes the reporter a good candidate for new, and even more interesting, applications such as flow cytometry or dynamic fluorometry.

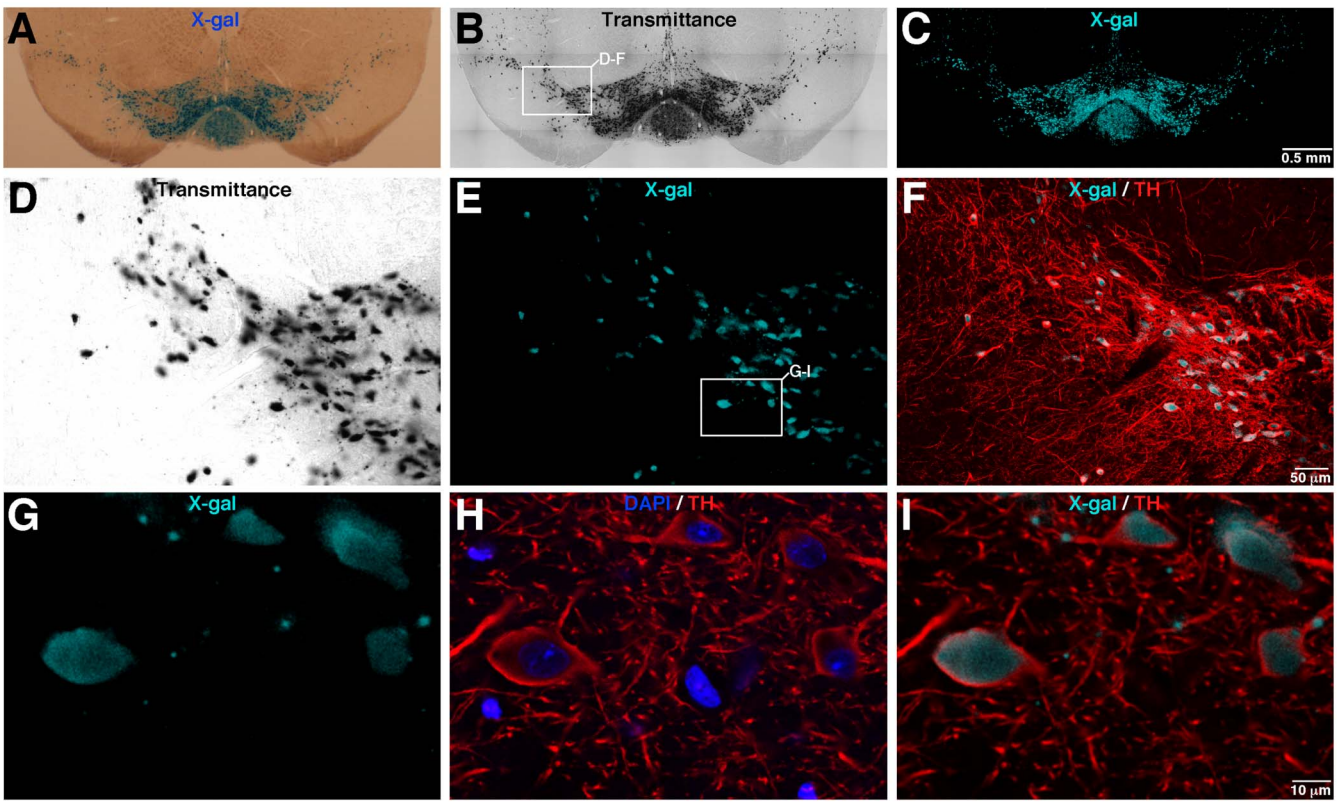

Figure 5 | Fluorescence confocal acquisition from X-gal staining using the high LacZ expression TH-ires-Cre/R26R reporter mouse line. (A–C), Brain coronal section of a TH-ires-Cre/R26R mouse showing high level of X-gal staining on the dopaminergic mesencephalic neurons, visualized by classical light transmitted microscopy (A), transmitted microscopy after 633 nm illumination (B) and by fluorescence X-gal confocal acquisition (C). (D–F), images corresponding with the inset marked in B, showing the transmittance (D, after 633 nm illumination), X-gal fluorescence (E) and X-gal/TH fluorescence merged signal (D, after TH inmufluorescence). (G–I), High magnification pictures of the area labelled by the inset in panel E, illustrating the X-gal fluorescence (G) and DAPI/TH (H) or X-gal/TH (I) merged images. Images reported in B and C were acquired using the mosaic function (with a 20× objective) of the confocal microscope. Confocal adquisition from a 12.0 µm Z-stack, voxel depth of 0.498 µm and pinhole airy 1.23.

Methods

Animals. Most of the experiments were carried out with heterozygous GDNF/LacZ mice[6,7]. In addition, confocal acquisition of fluorescence from X-gal staining was also performed on TH-ires-Cre/R26R mouse. All experiments were performed according to the animal care guidelines of the Council of the European Union (86/609/EEC), and were approved by the Animal Research Committee of the University Hospital Virgen del Rocío (University of Seville).

Purification and absorption/emission spectra of X-gal. *E. coli* (DH5α) expressing β-galactosidase and controls (without β-galactosidase expression) were grown overnight at 37°C in Luria broth media (Invitrogen) with 100 μg/ml ampicillin, 0.5 mM isopropyl-β-D-1-thiogalactopyranoside (IPTG) and 80 μg/ml X-gal. Bacteria were harvested by centrifugation at 16000 g for 2 min and were lysed with P1 lysis buffer (Quiagen). Cell extracts were centrifuged at 16000 × g for 2 min, the supernatants were discarded and the blue precipitate was collected, resuspended in 70% (v/v) perchloric acid and incubated at 22°C for 15 min. Thereafter, the suspensions were centrifuged at 16000 g for 5 min at 4°C, the precipitate suspended in PBS and deposited on a coverslip, and images obtained as shown in Fig. 1C and D. The emission spectrum was also obtained by a λ scan method on a Leica TCS SP2 confocal microscope (Fig. 1B). To obtain the absorption spectrum, the X-gal precipitate was dissolved with 0.1 N NaOH and analysed on an ultraviolet-visible spectrophotometer (Beckman DU 640; Beckman), with the suspension obtained from the control bacteria (without β-galactosidase expression) used as blank.

Histology. After transcardial perfusion of mice with 50 ml of PBS (Sigma) and 50 ml of 4% paraformaldehyde (Sigma) in PBS at 37°C, brains were immediately removed and fixed for 2–3 hours at 4°C with 4% paraformaldehyde in PBS. Coronal sections (thickness 30–50 μm) were cut with a cryostat (Leica) or vibratome (Leica). X-gal staining was performed on sections from GDNF/Lacz heterozygous mice[6,7] or TH-ires-Cre/R26R mice. Briefly, brain coronal sections were washed 3 times in solution C (137 mM NaCl, 2.7 mM KCl, 10 mM Na_2HPO_4, 2 mM KH_2PO_4, 2 mM $MgCl_2$, 5 mM EGTA, 0.02% IGEPAL, 0.01% Na desoxycholate) and incubated overnight on X-gal staining solution (solution C + 10 mM K_3FeCN_6, 10 mM K_4FeCN_6, 0.5 mg/ml X-gal). After X-gal staining, immunofluorescence detection was performed as previously described[7] for glial fibrillary acid protein (GFAP; 1 : 500; Dako), parvalbumin (1 : 5000, Swant) and DARPP32 (1 : 200, Millipore). Anti-mouse IgG conjugated with Alexa Fluor488 or anti-rabbit IgG conjugated with Alexa Fluor568 (1 : 400; Invitrogen) were used as secondary antibodies. Nuclei were stained with DAPI (1 : 1000; Sigma). Brain sections were mounted with Dako fluorescence mounting medium (Dako) or Vectashield fluorescence mounting medium (Vector). Transmitted light images (left panel in Figure 2A) were obtained using an Olympus AX70 microscope with a DP72 refrigerated digital camera. Confocal images were acquired using a Leica TCS SP2 confocal microscope.

Confocal acquisition and optic correction method. Direct confocal acquisition of fluorescence was performed using a Leica TCS SP2 microscope (Leica) equipped with a Blue-diode 405 nm, Argon-Krypton 458–514 nm, Helium-Neon 543 nm, and Helium-Neon 633 nm lasers. Most of the images were acquired using a HCX Pl Apo 20×/0.70 or HCX Pl Apo CS 63×/1.3 immersion objectives. Tissue sections were excited at 633 nm with the Helium-Neon 633 nm laser, and the transmittance signal and the fluorescence signal (recorded at 650–770 nm) were visualized to adjust the gain of the fluorescence photomultiplier until a clear fluorescence signal coincident with the X-gal precipitates (which are simultaneously visualized via the light transmitted channel) was obtained. Once the optimal gain of the fluorescence photomultiplier had been determined, both the fluorescence emission (650–770 nm) and the transmittance signal were recorded on a specific Z-stack. Fluorescence and transmitted light images were digitized with an 8-bit scale and their values were obtained with the appropriate confocal microscope software tools (Leica TCS SP2). The transmittance values were subtracted from the fluorescence images on each confocal plane, and the resulting X-gal fluorescence images (transmittance subtracted) were stored. The blur filter (3 × 3) was applied to most of our X-gal fluorescent images. This image processing filters the high frequencies out of the image, reducing the distinctive transitions from low to high intensity values (Supplementary Fig. 2–4 show a complete set of images illustrating the whole X-gal fluorescence image processing). Thereafter, confocal acquisition of the additional fluorescence labels was performed as follows: DAPI (excited at 405 nm and recorded on 415–450 nm), GFAP-Alexa 488 nm (excited at 488 nm and recorded at 515–550 nm), and parvalbumin-Alexa 568 nm (excited at 561 nm and recorded at 575–620 nm).

1. Soriano, P. Generalized lacZ expression with the ROSA26 Cre reporter strain. *Nat. Genet.* **21**, 70–71 (1999).
2. Silhavy, T. J. & Beckwith, J. R. Uses of lac fusions for the study of biological problems. *Microbiol. Rev.* **49**, 398–418 (1985).
3. Pereira, F. A. [Whole-mount histochemical detection of beta-galactosidase activity]. *Curr. Protoc. Mol. Biol.* [14.14.1–14.14.8] (Wiley, New York, 2001).
4. Seymour, P. A. & Sander, M. Immunohistochemical Detection of β-Galactosidase or Green Fluorescent Protein on Tissue Sections. *Methods Mol. Biol.* **411**, 13–23 (2007).
5. Burn, S. F. Detection of β-galactosidase activity: X-gal staining. *Methods Mol. Biol.* **886**, 241–250 (2012).
6. Sánchez, M. P. *et al.* Renal agenesis and the absence of enteric neurons in mice lacking GDNF. *Nature* **382**, 70–73 (1996).
7. Villadiego, J. *et al.* Selective glial cell line-derived neurotrophic factor production in adult dopaminergic carotid body cells in situ and after intrastriatal transplantation. *J. Neurosci.* **25**, 4091–4098 (2005).
8. Schönenbrücher, H. *et al.* Fluorescence-based method, exploiting lipofuscin, for real-time detection of central nervous system tissues on bovine carcasses. *J. Agric. Food Chem.* **56**, 6220–6226 (2008).
9. Hidalgo-Figueroa, M., Bonilla, S., Gutiérrez, F., Pascual, A. & López-Barneo, J. GDNF is predominantly expressed in the PV+ neostriatal interneuronal ensemble in normal mouse and after injury of the nigrostriatal pathway. *J. Neurosci.* **32**, 864–872 (2012).
10. Pascual, A. *et al.* Absolute requirement of GDNF for adult catecholaminergic neuron survival. *Nat. Neurosci.* **11**, 755–761 (2008).
11. Muñoz-Manchado, A. *et al.* Neuroprotective and reparative effects of carotid body grafts in a chronic MPTP model of Parkinson's disease. *Neurobiol. Aging* **34**, 902–915 (2013).
12. Matei, V. A. *et al.* Near-infrared laser illumination transforms the fluorescence absorbing X-Gal reaction product BCI into a transparent, yet brightly fluorescent substance. *Brain Res. Bull.* **70**, 33–43 (2006).
13. Dimri, G. P. *et al.* A biomarker that identifies senescent human cells in culture and in aging skin in vivo. *Proc. Natl. Acad. Sci. U.S.A.* **92**, 9363–9367 (1995).

Acknowledgments

We thank A.M. Muñoz-Cabello for critical reading of the manuscript, to J.I. Piruat and B. Díaz-Castro for providing histological sections and images, and N. Suarez-Luna and A. Bermejo-Navas for help with the histology. Support was obtained from the Spanish Ministries of Economy and Innovation (SAF, FIS, Red TERCEL, and CIBERNED programs), the Andalusian Government, and the Botín Foundation.

Author contributions

K.L.L. and J.V. designed and performed the experiments. J.T.A. and J.L.B. supervised the project. J.V. and J.L.B. wrote the manuscript.

Additional information

Supplementary information accompanies this paper at http://www.nature.com/scientificreports

Competing financial interests: The authors declare no competing financial interests.

How to cite this article: Levitsky, K.L., Toledo-Aral, J.J., López-Barneo, J. & Villadiego, J. Direct confocal acquisition of fluorescence from X-gal staining on thick tissue sections. *Sci. Rep.* **3**, 2937; DOI:10.1038/srep02937 (2013).